

Communications

Fiber-Optic Sensor Simultaneously Detecting Localized Surface Plasmon Resonance and Surface-Enhanced Raman Scattering

Erdene Norov¹, Hyeon-Ho Jeong², Jae-Hyoung Park², Seung-Ki Lee² and Dae Hong Jeong^{1,3*}

¹ Interdisciplinary Program in Nano-Science and Nanotechnology, Seoul National University, Seoul 151-742, Korea

² Department of Electronics and Electrical Engineering, Dankook University, Gyeonggi-do 448-701, Korea

³ Department of Chemistry Education, Seoul National University, Seoul 151-742, Korea

ABSTRACT : This study reports a fiber-optic sensor detecting biomolecule by simultaneously monitoring localized surface plasmon resonance (LSPR) from gold nanoparticles (Au NPs) of *ca.* 50 ± 5 nm attached on one end of optical fiber and surface enhanced Raman scattering (SERS) of the reporter molecules adsorbed on the gold surfaces as an additional sensing tool. The sensor was fabricated by immobilizing Au NPs on one end of an optical fiber by chemical reaction. LSPR and SERS signals of the sensor were measured using various refractive indices solutions. Finally, the sensor was applied to observe real-time LSPR sensor-gram and SERS spectra of the reporter molecule of 4-aminophenol during the antibody-antigen reaction of interferon-gamma (IFN- γ) as a proof-concept experiment of biological applications.

Surface plasmon resonance (SPR) is recognized as a powerful tool for refractive index (RI) sensing. SPR has shown a great potential for biosensors, allowing real-time analysis of bio-specific interactions without labeling target molecules. However, most of the SPR instruments have very complex optical setups and they cannot be used for the multiplex assay.^{1,2} Localized surface Plasmon resonance (LSPR) monitoring collective oscillation of free electron localized in nanoparticles and nanometer-scale rough surfaces has been introduced as an alternative technique of SPR. Localized optical field near nanoparticle surfaces has

high sensitivity of refractive index change.³

Surface-enhanced Raman scattering (SERS) has been known as an optical phenomenon which monitors vibrational finger-prints of molecules adsorbed on specially fabricated surfaces of noble metals in a manner of single molecule sensitivity.^{4,5} It has shown a great potential as a multiplex bio-detection due to its highly narrow band-width compared with other optical methods such as fluorescence and SPR scattering.^{6,7}

LSPR can sensitively and quantitatively measure binding processes of the bio-molecular reactions and SERS can distinguish multiple analytes. Monitoring LSPR and SERS simultaneously can allow detection of bio-molecules sensitively and quantitatively for multiple target molecules. There have been a few reports that utilize SPR and SERS simultaneously.⁸⁻¹¹ However, since these setups are based on Kretschmann's configuration and require complex setups, there is a need for optical method that utilizes LSPR and SERS simultaneously with simple optical setup for portable and inexpensive applications. Use of fiber optic (FO) simplifies the optical setup and costs less.^{12,13} There have been a number of studies that collected the LSPR¹⁴⁻¹⁸ and SERS^{13,14,19} through optical fibers.

This study demonstrates a prototype of FO sensor utilizing LSPR and SERS simultaneously for a potential application to real-time detections of multiplexed biological systems. Gold nanoparticles were introduced on one end of an optical fiber for LSPR and SERS activity. LSPR sensitivity of the sensor was measured using various refractive indices solutions and SERS sensitivity was measured by

*To whom correspondence should be addressed.
E-mail: jeongdh@snu.ac.kr

obtaining the SERS spectrum of 4-aminothiophenol (ATP) as a SERS reporter molecule. Then, the LSPR sensor-gram and SERS spectra of FO sensor were measured simultaneously during the antibody-antigen reaction of interferon-gamma ($\text{IFN-}\gamma$)²⁰ and the correlation of both signals was analyzed as a proof-concept experiment for multiplex bio-detections.

EXPERIMENTAL SECTIONS

Optical system

Figure 1 shows a schematic diagram of a FO LSPR and SERS detection system. One part is for detection of LSPR and the other is for detection of SERS. The 647-nm laser-line from a tunable Kr-ion laser (Innova 300C) was used as an excitation light source for LSPR and SERS. One end of an optical fiber was open for light entrance and the other end was prepared for sensing area. The $\times 10$ objective lens (N.A. = 0.25, W.D. = 10.6 mm, Olympus) was used to collimate the laser lights into the optical fiber. The SERS signals were measured by a spectroscopy (Triax 320, JY-Horiba) equipped with a CCD detector (DU401, Andor Corp.) and the LSPR signals were measured by a photodiode detector (S121C, Thorlabs). The smooth line in Figure 1B indicates an incident light path into the optical fiber and the dashed line does a light path reflected from the sensor surface.

Chemicals

Gold(III) chloride trihydrate ($\text{HAuCl}_4 \cdot 3\text{H}_2\text{O}$, 99.9 %), 3-aminopropyl-dimethylethoxysilan (APMES, 97 %), trisodium citrate (99 %), 4-aminothiophenol (ATP, 97 %), bovine serum albumin (BSA, 10%), phosphate buffered saline (PBS, pH 7.4) were purchased from Sigma Aldrich, hydrogen peroxide (H_2O_2 , 30%), sulfuric acid (H_2SO_4 , 95%), methanol (99.5%), ethanol (99%) were supplied with analytical grade by Daejung Chemicals and borate buffer (pH 8.5) were supplied by GE Healthcare. Antibody interferon-gamma (Purified Anti-Human $\text{IFN-}\gamma$), and antigen interferon-gamma (Recombinant Human $\text{IFN-}\gamma$) were purchased from Becton Dickinson. The refractive index solutions were purchased from Cargille Labs (Series AAA). All the chemicals were used without further purification.

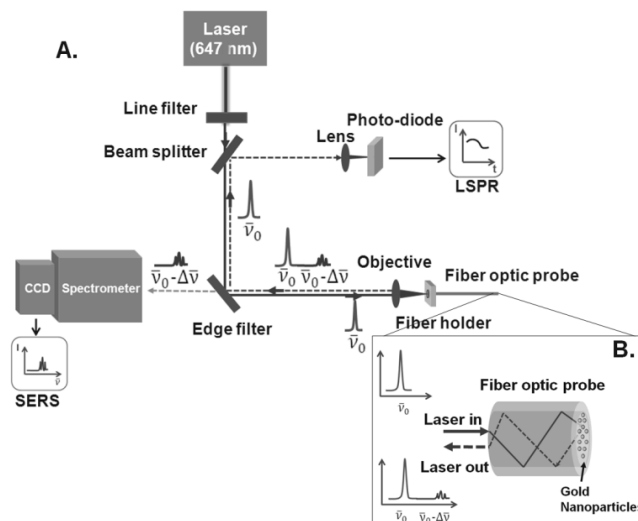


Figure 1. Schematics of optical path. (A) Schematic diagram of the LSPR and SERS simultaneous detection system used in the present study. (B) Zoomed-in image of the light traveling mechanism through the FO sensor probe.

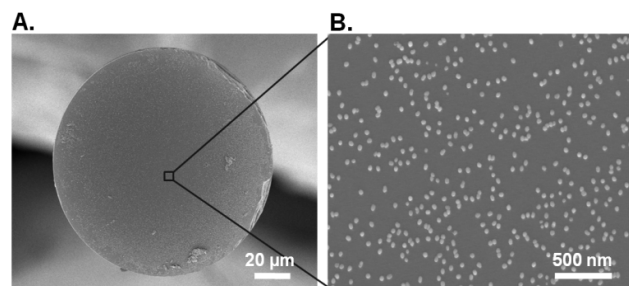


Figure 2. FE-SEM image of the FO sensor probe. (A) End-face of the FO sensor probe, and (B) the zoomed-in image.

A multimodal optical fiber of 105- μm core and 10- μm cladding was purchased from Thorlabs (AFS, 105/125Y). The protecting polymer at both ends of the optical fiber was removed and cleaved to expose smooth silica surface. Then, the end-face of the optical fiber was activated with hydroxyl functional groups by dipping into the piranha solution (a mixture of H_2SO_4 and 30 % H_2O_2 (3:1, v/v)) for 20 minutes at 95 °C for further silanization.

The FO was then immersed into 5% (v/v) APMES solution for 90 minutes to form a self-assembled monolayer (SAM) of APMES on the end-face of the optical fiber. Next, the optical fiber was immersed in

the gold colloid solution for 1 hour in order to immobilize the Au NPs on the end-face of the optical fiber.²¹ The FO sensor probe surface was then characterized by field emission scanning electron microscope (FE-SEM, SUPRA 55VP, Carl Zeiss). SEM images of the sensor surface of the FO probe shown in Figure 2, exhibits that the Au NPs were evenly introduced without heavy clustering of nanoparticles.

RESULT

Simultaneous measurement and FO sensor sensitivity

SPR signal is sensitive to the refractive index change around the gold nanoparticles attached on the end surface of the FO sensor. In order to use SERS signal to sense the refractive index change, ATP molecules are adsorbed on the gold surface since the SERS intensity of ATP depends on localized optical field due to surface plasmon resonance of gold nanoparticles.

LSPR and SERS signals from the sensor surface were measured for five solutions of different refractive indices (Series AAA, Cargille Labs), which were 1.34, 1.35, 1.36, 1.37 and 1.38. As a reference, signals from the FO sensor were measured for deionized water of which the refractive index is 1.33.

Figure 3 shows LSPR and SERS signals from the FO sensor that was measured simultaneously for five refractive index solutions. The 647-nm laser-line was used as an excitation light source for SERS as well as a light source for LSPR. Upper and the bottom insets show real-time measurement data of LSPR and SERS, respectively. Both SERS and LSPR signals increase linearly due to the refractive indices varying from 1.33 to 1.38.

To confirm the LSPR signal from the FO sensor, the resonance spectral change due to the refractive indices using white light were also measured as shown in supporting information Figure S1. The spectrum linearly increased with the refractive index which has the same tendency with laser-excitation measurement of the FO sensor.

The LSPR sensitivity is usually expressed using the intensity modulation, which measures the change of reflected light intensity (ΔI) per unit change of the refractive index (Δn) and expressed as $S = \Delta I / \Delta n$ (RIU⁻¹) as a function of normalized intensity. Therefore measured LSPR resonance intensity of FO sensor was

normalized with reference signal of deionized water which the refractive index is 1.33 and plotted against the refractive index change shown as Figure 3. Herein, RIU means refractive index unit and the slope was founded 13.107 RIU⁻¹.

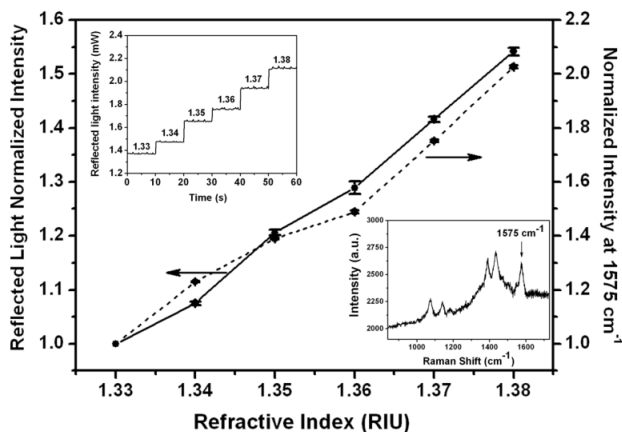


Figure 3. FO sensor simultaneous measurements with various refractive indices solutions. Upper inset shows real time sensor-gram with different refractive indices at wavelength 647 nm and the bottom inset shows the simultaneous measurement of ATP SERS spectrum.

Antibody IFN- γ immobilization

In order to investigate the possibility of detecting a biomolecular reaction, this sensor was used to monitor antibody-antigen reaction of IFN- γ . For this purpose Au NPs on the fiber surface was further immobilized with antibody of IFN- γ . Figure 4 illustrates schematic diagram of the immobilization process of antibody IFN- γ .

We have previously reported the procedure of antibody IFN- γ immobilization to FO sensor surface.^{16,17,18} Briefly, the FO sensor with gold nanoparticles on its surface was immersed into 100 μ l of 10⁻³ M ATP solution for 180 minutes in order to immobilization of SERS reporter molecule. Then FO sensor was immersed into 100 μ l of 20 μ g/ml antibody IFN- γ solution with borate buffer (pH 8.5) for 15 minutes. Herein, the antibody IFN- γ was immobilized on gold nanoparticles on the surface of the FO sensor. Finally, the FO sensor was immersed into 100 μ l of 1% BSA borate buffer (pH 8.5) solution for 15 minutes to prevent the nonspecific binding. Immobilization of antibody IFN- γ was monitored by simultaneous measurement of LSPR and SERS during antibody IFN- γ immobilization on the FO sensor.

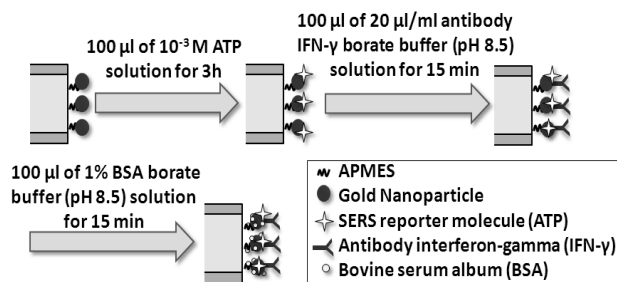


Figure 4. Schematic illustration of the antibody IFN- γ immobilization process.

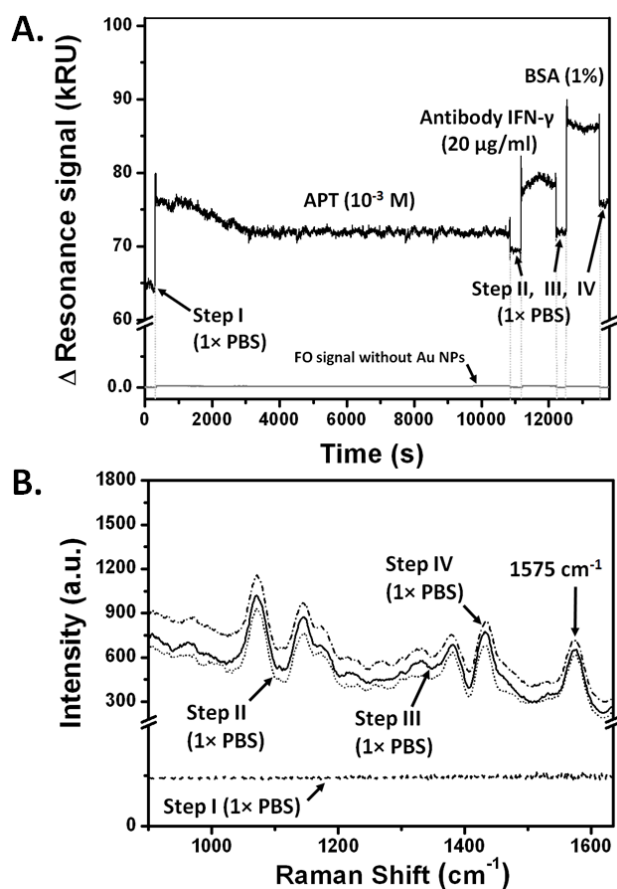


Figure 5. LSPR and SERS simultaneous measurements. (A) Real time sensor-gram of the LSPR scattering intensity by 647-nm photo-excitation during sequential immobilization processes of ATP reporter molecule, antibody IFN- γ and BSA. (B) Simultaneous measured ATP SERS spectrum during the immobilization process.

Figure 5A shows a real-time sensor-gram of LSPR scattering intensity by 647-nm photo-excitation during sequential immobilization processes of ATP reporter molecule, antibody IFN- γ and BSA. The observed intensity change at 647-nm during the immobilization

process was converted to unit change of refractive index RIU ($\Delta n = \Delta I/S$) following the definition of Biacore²², in which 0.001 RIU corresponds to 1000 Resonance unit (RU)

The sensor-gram was composed of four step measurements in phosphate buffered saline (PBS, pH 7.4) for 5 minutes between every sequential immobilization processes in order to recognize the optical change on the FO sensor surface.

Before the ATP reporter molecule treatment FO sensor was used to measure resonance intensities in phosphate buffered saline (PBS, pH 7.4) and used as a baseline which corresponds to step I. Step II, III and IV correspond to the resonance intensity measurements after ATP, antibody IFN- γ and BSA immobilization, respectively. The resonance intensities showed step-wise increase from step I to IV.

For comparison, we also measured resonance intensities during the whole immobilization processes using FO without Au NPs, which is shown as a grey line in the real-time sensor-gram. Intensity values were almost constant, indicating that there was little change in refractive index near the surface of the FO sensor.

Figure 5B shows simultaneous measurement of SERS spectra of ATP reporter molecule during the immobilization process of ATP, antibody IFN- γ and BSA. Dashed, dotted, solid and dot-dashed lines correspond to I, II, III and IV steps, respectively. SERS intensities of ATP depend on localized optical field due to surface plasmon resonance of gold nanoparticles. Therefore, SERS intensities of ATP were increased from measurement step I to step IV, which have the similar tendency of measured LSPR scattering intensity shown in Figure 5A.

Real-time detection of antibody-antigen reaction of IFN- γ

Figure 6A shows a real-time sensor-gram of the LSPR scattering intensity at 647-nm excitation. The LSPR scattering intensity was converted to Resonance unit (RU). Before injecting the antigen of IFN- γ , the FO sensor was used to measure LSPR scattering intensities in phosphate buffered saline (PBS, pH 7.4) for 3 minutes and used as a baseline. Next, 10 ng/ml of antigen IFN- γ was injected and LSPR scattering signal was recorded for 12 minutes. Once the antigen was injected, the scattering signal increased drastically and then remained constant, showing average intensity of 4.57 ± 0.13 kRU. Finally, phosphate buffered saline (PBS, pH 7.4) was injected in order to remove nonspecific binding of antigen of IFN- γ . LSPR scattering intensity was recorded for 24 minutes until the signal was stabilized. The measured signal was

1.49 ± 0.11 kRU.

SERS signals were simultaneously measured before and after bio-reaction. The measurement points were indicated in Figure 6A. Figure 6B illustrates the SERS spectra before and after the antibody-antigen reaction. The solid and dotted lines correspond to SERS spectrum of ATP from FO sensor in phosphate buffered saline (PBS, pH 7.4) before and after antigen injection, respectively. After the bio-reaction of IFN- γ the SERS spectrum of the ATP became more intense due to a binding between antibody and antigen of IFN- γ .

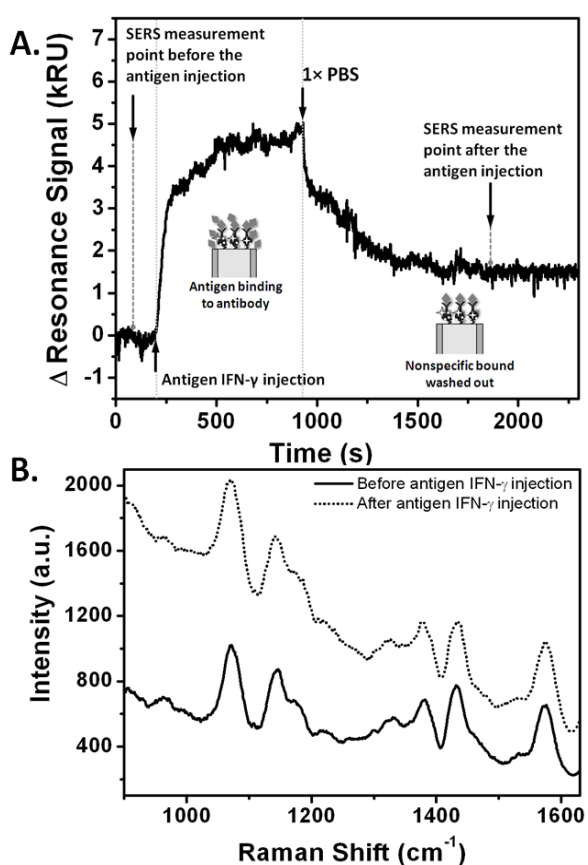


Figure 6. Simultaneous measurements of the LSPR and SERS during the antibody-antigen reaction of IFN- γ . (A) A real-time sensor-gram of the resonance intensity at 647-nm excitation. (B) Simultaneously measured SERS spectrum of ATP during the antibody-antigen reaction of IFN- γ .

LSPR can sensitively and quantitatively measure binding processes of the bio-molecular reactions. However, LSPR cannot distinguish multiple targets in one time. SERS has a great potential as a multiplex bio-detection due to its highly narrow band-width compared with other optical methods such as fluorescence and

SPR scattering. Monitoring LSPR and SERS simultaneously can detect bio-molecules sensitively and quantitatively for multiple target molecules. For example, there are multiple capture antibodies on the FO sensor surface with specific reporter molecules, observed SERS spectrum change can distinguish which specific binding of antigen is involved. The result of this study presents a proof-of-concept in such application of LSPR and SERS for multiple bio-detections.

CONCLUSIONS

In this study, we have demonstrated FO LSPR and SERS simultaneous sensor that has a unique ability to detect real-time sensing of molecular binding. The sensor was fabricated using Au NPs and the sensitivity of the FO sensor was defined to measure various refractive index solutions in order to detect antibody-antigen reaction of IFN- γ . The response of the observed real-time sensor-gram exhibited target binding events. In a multiplexing assay, LSPR sensor-gram can show the real-time binding process and the SERS signal can differentiate which target was targeted and monitored. The concept and method demonstrated in this study can serve as a basis for developing multiplex assays for the detection of molecular binding events in biological systems.

KEYWORDS : Fiber-Optic Sensor, Localized Surface Plasmon Resonance, Surface Enhanced Raman Scattering, Simultaneous detection, Gold Nanoparticles

Received June 16, 2013; Accepted July 15, 2013

ACKNOWLEDGEMENT

This research was supported by the Pioneer Research Center Program through the National Research Foundation of Korea funded by the Ministry of Science, ICT & Future Planning (NRF-2011-0027888).

SUPPORTING INFORMATION

Experimental procedures: FO sensor with white light measurement. This material is available free of charge via the Internet at <http://photos.or.kr>

REFERENCES AND NOTES

- Homola, J.; Yee, S. S.; Gauglitz, G. *Sens. Actuat. B Chem.* **1999**, *54*, 3-15.
- Homola, J. *Chem. Rev.* **2008**, *108*, 462-493.
- Hutter, E.; Fendler, J. H. *Adv. Mater.* **2004**, *16*, 1685-1706.
- Zhao, J.; Zhang, X. Y.; Yonzon, C. R.; Haes, A. J.; Van Duyne, R. P. *Nanomedicine.* **2006**, *1*, 219-228.

5. Willets, K. A.; Van Duyne, R. P. *Annu. Rev. Phys. Chem.* **2007**, *58*, 267-97.
6. Sepulveda, B.; Angelome, P. C.; Lechuga, L. M.; Liz-Marzan, L. M. *Nano Today* **2009**, *4*, 244-251.
7. Campion, A.; Kambhampati, P. *Chem. Soc. Rev.* **1998**, *27*, 241-250.
8. Liu, Y.; Xu, S. P.; Tang, B.; Wang, Y.; Zhou, J.; Zheng, X. L.; Zhao, B.; Xu, W. Q. *Rev. Sci. Instrum* **2010**, *81*, 036105:1-3.
9. Meyer, S. A.; Le Ru, E. C.; Etchegoin, P. G. *Anal. Chem.* **2011**, *83*, 2337-2344.
10. Xuan, X. Y.; Xu, S. P.; Liu, Y.; Li, H. B.; Xu, W. Q.; Lombardi, J. R. *J. Phys. Chem. Lett.* **2012**, *3*, 2773-2778.
11. Fu, C. C.; Hu, C. X.; Liu, Y.; Xu, S. P.; Xu, W. Q. *Anal. Methods-Uk* **2012**, *4*, 3107-3110.
12. Stoddart, P. R.; White, D. J. *Anal. Bioanal. Chem.* **2009**, *394*, 1761-1774.
13. Fan, X. D.; White, I. M.; Shopoua, S. I.; Zhu, H. Y.; Suter, J. D.; Sun, Y. Z. *Anal. Chim. Acta.* **2008**, *620*, 8-26.
14. Jorgenson, R. C.; Yee, S. S. *Sens. Acuat. B Chem.* **1993**, *12*, 213-220.
15. Mitsui, K.; Handa, Y.; Kajikawa, K. *Appl. Phys. Lett.* **2004**, *85*, 4231-4233.
16. Jeong, H. H.; Erdene, N.; Lee, S. K.; Jeong, D. H.; Park, J. H. *Opt. Eng.* **2011**, *50*, 124405:1-8.
17. Jeong, H. H.; Erdene, N.; Park, J. H.; Jeong, D. H.; Lee, H. Y.; Lee, S. K. *Biosens. Bioelectron.* **2013**, *39*, 346-351.
18. Jeong, H. H.; Erdene, N.; Park, J. H.; Jeong, D. H.; Lee, S. K. *J. Nanosci. Nanotechnol.* **2012**, *12*, 7815-7821.
19. Lee, B.; Roh, S.; Park, J. *Opt. Fiber Technol.* **2009**, *15*, 209-221.
20. Schroder, K.; Hertzog, P. J.; Ravasi, T.; Hume, D. A. *J. Leukocyte Biol.* **2004**, *75*, 163-189.
21. Lee, H.; Kim, H. J.; Park, J. H.; Jeong, D. H.; Lee, S. K. *Meas. Sci. Technol.* **2010**, *21*, 1-9.
22. Nagata, K.; Handa, H. *Real-Time Analysis of Biomolecular Interactions Applications of Biacore* **2000**, Springer-Verlag, New York.